Research article

AI model to detect contact relationship between maxillary sinus and posterior teeth

Wanghui Ding [a,*], Yindi Jiang [b,1], Gaozhi Pang [c,1], Ziang Liu [a], Yuefan Wu [a], Jianhua Li [d,**], Fuli Wu [c,***]

[a] *Stomatology Hospital, School of Stomatology, Zhejiang University School of Medicine, Zhejiang Provincial Clinical Research Center for Oral Diseases, Key Laboratory of Oral Biomedical Research of Zhejiang Province, Cancer Center of Zhejiang University, Hangzhou, China*
[b] *Hangzhou Linping Traditional Chinese Medicine Hospital, China*
[c] *College of Computer Science and Technology, Zhejiang University of Technology, China*
[d] *Hangzhou Dental Hospital, China*

ABSTRACT

Objectives: To establish a novel deep learning networks (MSF-MPTnet) based on panoramic radiographs (PRs) for automatic assessment of relationship between maxillary sinus floor (MSF) and maxillary posterior teeth (MPT), and to compare accuracy of MSF-MPTnet, dentists and radiologists identifying contact relationship.
Study design: A total of 1035 PRs and 1035 Cone-beam computed tomographys（CBCT）images were collected from January 2018 to April 2022. The relationships were classified into class I and II by CBCT. Class I represents non-contact group, and class II represents contact group. 350 PRs were randomly selected as test dataset and accuracy of MSF-MPTnet, dentists, and radiologists was compared.
Results: The intraclass correlation coefficient of dentists was 0.460–0.690 and it was 0.453–0.664 for radiologists. Sensitivity and accuracy of MSF-MPTnet were 0.682–0.852and 0.890–0.951, indicating that the output performance of MSF-MPTnet was reliable. Accuracy of maxillary premolars and molars were 79.7%–90.3 %, 76.2%–89.2 % and 72.9%–88.3 % in MSF-MPTnet model, dentists and radiologists. Accuracy of class I relationship in the MSF-MPTnet model (67.7%–94.6 %) was higher than that of dentists (56.5%–84.6 %) in maxillary first premolars and right second premolar, and accuracy of class I relationship in the MSF-MPTnet model is also higher than radiologists (40.0%–78.1 %) in all teeth positions ($p < 0.05$).
Conclusions: MSF-MPTnet model could increase detecting accuracy of the relationship between MSF and MPT, minimize pseudo contact relationship and reduce frequency of CBCT use.

1. Introduction

Maxillary sinus (MS) is an important anatomic structure, which is the largest pyramid-shaped bilateral paranasal air sinus located

in the body of the maxilla [1]. The close relationship of the maxillary posterior teeth (MPT) and MSF may result in various complications. dental diseases including periapical or periodontal infections of MPT can spread to the MS and lead to odontogenic sinusitis, and it was found that over 50 % of maxillary sinusitis was of dental etiology [2,3]. In addition, tooth extraction or endodontic surgery can lead to perforation, formation of oroantral fistula, or root displacement into the MS [4]. Root protrusion into MS may induce root resorption or tipping during orthodontic treatment [5]. Therefore, accurate assessment of anatomic relationship between MSF and the root apexes of MPT is of clinical importance in diagnosing and treatment planning in the maxillary posterior area.

CBCT can be used to evaluate the 3-dimensional relationship between MSF and MPT, However, accessibility of CBCT is limited because the cost and radiation dose from CBCT are much higher than panoramic radiographs, and data loading and reading are time-consuming [6,7]. Panoramic radiographs, (PRs), is commonly used to evaluate the anatomic relationship between MSF and MPT because of their intrinsic advantages [8]. PRs have many advantages including short time for the procedure, greater patient acceptance and cooperation, overall coverage of the dental arches and associated structures, simplicity, low patient radiation dose and low cost [1]. However, there are some limitations such as superimposition of anatomic structures, distortion, and the absence of cross-sectional information, which will cause the pseudo-contact relationship between MSF and MPT. In addition, it takes dentists and radiologists more times to identify the relationship between MSF and MPT with the naked eye, and the accuracy should be improved.

Machine learning is a subgroup of AI which enhances automated learning ability without being distinctly programmed, and a popular field in machine learning is deep learning, which includes convolutional neural networks (CNN) and artificial neural networks (ANNs) [9]. DenseNet, a convolutional neural network with dense connectivity structure, is able to learn deeper and more discriminative features from images and has been applied to medical image analysis and has achieved breakthroughs. DenseNet requires fewer parameters and less computation to achieve state-of-the-art performance, and can learn more compact and more accurate models. DenseNet introduces a dense connection structure, connecting each layer directly to all subsequent layers, facilitating fuller information transmission. This mitigates gradient disappearance problems, accelerates training convergence, and improves network performance. DenseNet has been shown to significantly improve performance, particularly for tasks such as image segmentation and classification. Howerver, DenseNet may have higher computing resource requirements than some lightweight network architectures, especially in resource-constrained environments. Due to the densely connected structure, DenseNet needs to store more intermediate feature maps, this may result in a large memory footprint, unsuitable for some resource-constrained devices. Deep learning plays an important role in dentistry for patient diagnosis, clinical decision making, and prediction of dental failures in the field of oral and maxillofacial surgery, restorative dentistry, prosthodontics, orthodontics, endodontics, forensic dentistry, radiology, and periodontics [10–13]. The automatic detection and segmentation of teeth and MS structure in PRs have been reported in the literature, indicating that deep learning-based artificial intelligence models can perform panoptic segmentation of images, including those of the MS and teeth [13–15]. Currently, artificial intelligence is widely applied in the field of the maxillary sinus, including 3D automatic segmentation of the maxillary sinus on CBCT [16], automatic detection and segmentation of morphological changes in the maxillary sinus
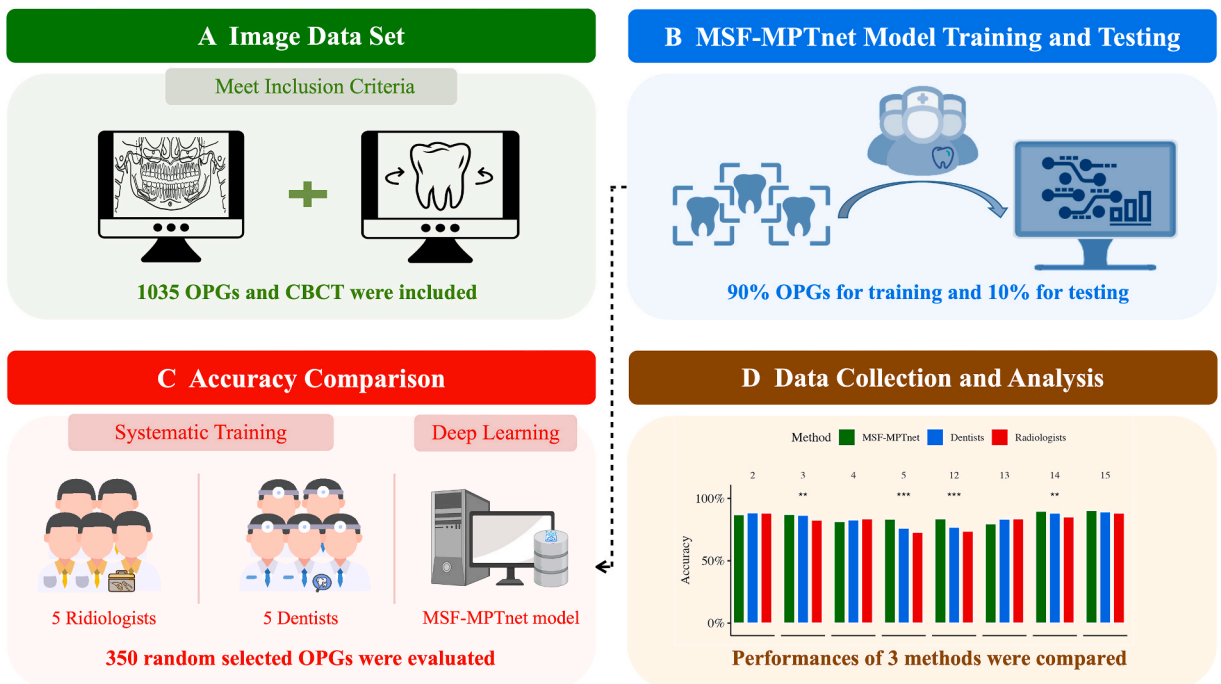

Fig. 1. Study protocol. A.A total of 1035 PRs and CBCT images which meet the inclusion criteria were collected. B.70 % PRs were used for training and 30 % for testing. C.350 PRs were randomly selected as the test dataset and 5 dentists and 5 radiologists were asked to evaluate the dataset. D. Performances of 3 methods were compared.

mucosa based on three-dimensional convolutional neural networks on cone-beam CT images [17], and deep learning for detecting normal maxillary sinuses and maxillary sinus diseases on panoramic images [18]. However, there has been no study on using deep learning in PR to determine the actual contact relationship between MSF and MPT. The automatic detection of the relationship is very important in early warning of close contact between MSF and MPT to reduce the possible complications of dental therapy and reduce the CBCT use.

2. Materials and methods

This study was approved by the Ethic Committee of Stomatology Hospital, School of Stomatology, Zhejiang University School of Medicine (R20220129), and was conducted in compliance with the ICH-GCP principles and the Declaration of Helsinki (2013). The protocol of this study was shown in Fig. 1.

3. Image data set

This study was conducted at the Stomatology Hospital, School of Stomatology, Zhejiang University School of Medicine. The inclusion criteria: 1.patient age≥18 years; 2.maxillary posterior teeth (MPT) were intact without dental disease; 3.PRs and CBCT taken within 6 months for the same patient with no obvious artifacts. The exclusion criteria: patients have experienced orthodontic treatment, or experienced traumatic injury that disturbs the normal anatomy of MS. PRs were obtained by Orthophos 5OS Ceph (Dentsply Sirona, Bensheim, Germany) and CBCT was obtained by a 3D CBCT scanner NewTom VGi (QR S.R.L.,Verona, Italy). The CBCT data was acquired with a large field of view (FOV), with dimension greater than 15*15 cm. The tube voltage was set at 110 kV, and the current was adjustable. The exposure time for the acquisition was 1.8 s.

A total of 1035 PRs and 1035 CBCT images were collected from January 2018 to April 2022 form individuals aged 18–59 years. Informed consents were obtained from the patients for the publication of their image date. A dentist with five years of experience was trained to identify and record the relationship between MPT and MSF on CBCT. In this study, CBCT was considered as the gold standard for diagnosis. These images were divided into two categories: Class I represented the non-contact group, while Class II represented the contact group. All CBCT date were recorded by the same dentist twice within 3 months to verify its accuracy. The intra-class correlation coefficient of the dentist was 0.948, indicating excellent accuracy of annotation between the two instances.

Subsequently, by randomly selecting 350 PRs as a test dataset and using the CBCT analysis results as the gold standard, the accuracy of the MSF-MPTnet, dentists, and radiologists were computed and compared. This process was carried out to evaluate the performance of the MSF-MPTnet in the relevant tasks.

All the participants agreed to have their images published. Using the true contact relationships between MSF and MPT on CBCT as the gold standard, the vertical relationship between MSF and MPT could be divided into two classes: (1) Class I: MPT not in contact with MSF, which means the root apexes extending below/outside the MS; (2) Class II: MPT in contact with MSF, which means the root apexes contacting with or extending above/inside the MS (Fig. 2A).

4. Deep learning network construction and training

The core mechanism of contact detection revolves around a deep learning network known as DenseNet. This network has demonstrated outstanding accuracy and high-speed analysis in the detection of regions of interest (ROI). Its densely connected design
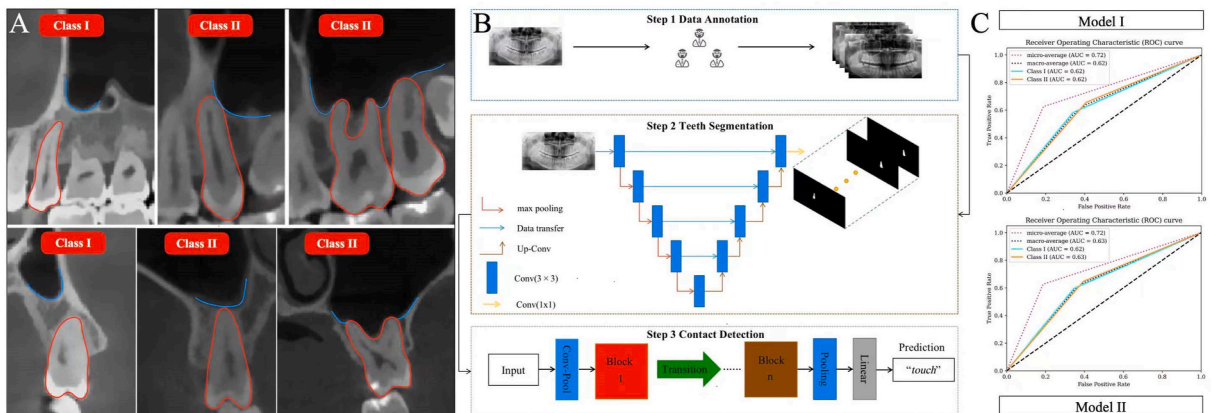

Fig. 2. The workflow of MSF-MPTnet model was reliable. A.The demonstration of class I and class II relationship of MSF and MPT in sagittal and coronal dimension. The blue curve represents the MSF, and the contour of premolars and molars represents MPT B.The workflow of MSF-MPTnet model includes data annotation, teeth segmentation and contact detection. In step 3, the layers between two dense blocks are referred to as transition layers and change feature-map sizes via convolution and pooling C. The receiver operating characteristic curves (ROC) illustrate the model performance of the convolutional neural network is reliable.

facilitates more comprehensive feature propagation within the network, aiding in better capturing both local and global information in images. Furthermore, the use of transition layers effectively controls the number of feature maps, alleviating the computational burden on the network and enhancing processing speed. These characteristics contribute to the exceptional performance and efficient analysis speed of DenseNet in contact detection tasks.

The workflow of the model could be divided into the following three stages (Fig. 2B), Initially, during the data annotation phase, we adjusted the resolution of panoramic X-ray photos, enhancing it to 2440*1280 pixels. By detecting contact between the maxillary sinus and teeth in CBCT images, we categorized them into contact groups and utilized the open-source software 3D-Slicer to delineate the maxillary sinus lines on both the left and right sides. The experiment encompassed a total of 1035 panoramic radiographs. We partitioned the dataset in an 7:3 ratio, randomly distributing images between the training set (n = 685) and the test set (n = 350).

Next, in our experiments, we implemented a series of data augmentation techniques on the training set to enhance the robustness and generalization ability of the model. The following data augmentation operations were applied:

Mirror flipping: We diversified the data further by employing mirror flipping operations. By simulating different directions of mirror symmetry, we ensured the model's resilience when handling images from various perspectives and orientations.

Gamma transformation: To enhance contrast and brightness variations in the images, we employed gamma transformation. By adjusting the grayscale levels, we could capture subtle details in the organizational structure. The gamma transformation was configured within the range of 0.7–1.5 to ensure moderate adjustments to the images, thereby strengthening the model's adaptability to different brightness conditions.

By implementing these data augmentation operations, we expanded the size of the training dataset, generating approximately 2100 training samples in total. This augmentation significantly increased the diversity of training examples, contributing to the enhancement of the model's generalization ability and its capability to handle various image conditions and variations.

Furthermore, we proceeded with tooth segmentation. At this stage, we employed the Unet network for image processing, consisting of symmetric contraction and expansion paths. Specifically, the feature extraction part involved processing images through a downsampling module (Conv(3×3) + Conv(3×3) + Max Pooling(2×2)), generating five feature maps with an increased number of channels. The feature fusion part included processing images through an upsampling module (up-Conv + Conv(3×3) + Conv(3×3)), followed by deconvolution, feature map fusion, and convolution layers. Ultimately, a 1x1 convolution layer was utilized to output a vector containing probability scores for each pixel corresponding to each classification.

In the final stage of contact detection, we fed the images into DenseNet. DenseNet consists of multiple densely connected blocks and transition layers. The dense blocks contain layers such as BN + ReLU + Conv(1×1) + BN + ReLU + Conv(3×3), aimed at extracting rich feature information from the input images. Between two Dense Blocks, a transition layer is used with BN + Conv(1×1) + Average Pooling(2×2), effectively reducing the number of feature map inputs and optimizing the overall network structure. This design enables DenseNet to handle contact detection tasks more effectively, enhancing the system's performance.

4.1. Diagnostic performance analysis

To compare the accuracy among the dentists, the radiologists and the MSF-MPTnet automatic detection model. 350 PRs were randomly selected as the test dataset and 5 dentists (Dentist1-5) and 5 radiologists (Radiologist1-5) were asked to evaluate the dataset. Both of the dentists and radiologists received systematic training. The average accuracy of the dentists and radiologists for each tooth position was calculated, and and the accuracy was compared within each group. The accuracy of each tooth position was compared with the MSF-MPTnet detection model. Overall performance of the model outputs was verified using confusion matrices, accuracy (TP + TN)/(TP + FN + FP + TN), Precision (TP/(TP + FP)), recall (TP/(TP + FN)), F1 score (2Precision*Recall/(precision + Recall)), and average precision (AP = 01p(r)dr) were used to calculate the model diagnostic accuracy.

Table 1
Number of OPGs and CBCT included in different teeth positions and distribution of the relationship between MPT and MSF on CBCT.

Teeth position	2(upper right second molar)	3(upper right first molar)	4 (upper right second premolar)	5(upper right first premolar)	12(upper left first premolar)	13(upper left second premolar)	14(upper left first molar)	15(upper left second molar)
Number	1022	1024	1006	1009	1016	1016	1022	1021
Class I	199 (19.47 %)	248 (24.22 %)	471 (46.82 %)	820 (81.27 %)	822 (80.91 %)	464 (45.67 %)	238 (23.29 %)	185 (18.12 %)
Class II	823 (80.53 %)	776 (75.78 %)	535 (53.18 %)	189 (18.73 %)	194 (19.09 %)	552 (54.33 %)	784 (76.71 %)	836 (81.88 %)
ICC (intraclass correlation coefficient) of Dentists	0.551	0.587	0.588	0.460	0.548	0.665	0.690	0.593
ICC (intraclass correlation coefficient) of Radiologists	0.644	0.587	0.660	0.453	0.509	0.651	0.664	0.635

5. Statistical analysis

Chi-square test (sample size >5) or Fisher exact test (sample size ≤5) was used to compare the accuracy, and fisher's exact test is suitable when the expected values in any of the cells of a contingency table are below 5. IBM SPSS Statistics 26.0 was used for statistical analysis, and the significance level was set at $p < 0.05$ when comparing the three groups. The significant level was set at $p < 0.0167$ (0.05/3) when comparing two groups among the three groups. Intraclass correlation analysis was applied to assess interobserver agreement among the dentists and radiologists using the intraclass correlation coefficient (ICC).

6. Results

6.1. Number of X-rays included in different teeth positions and distribution of the relationship between MPT and MSF on CBCT

In total, there are 1035 X-rays included in this study. Some teeth that were not clear enough in PRs were excluded. Therefore, the number of PRs and CBCT collected for each tooth was not identical, as shown in Table 1. The number of teeth 2 (upper right second molar), 3 (upper right first molar), 4 (upper right second premolar), 5 (upper right first premolar), 12 (upper left first premolar), 13 (upper left second premolar), 14 (upper left first molar), 15 (upper left second molar) included was 1022, 1024, 1006, 1009, 1016, 1016, 1022, 1021 respectively.

Distribution of the relationship between MPT and MSF on CBCT was shown in Table 1. Class II relationships were the most common in maxillary molars, and class I relationships were the most common in maxillary first premolars. The percentage of class I and II was nearly equal in maxillary second premolars. The percentage of class I for teeth 2, 3, 4, 5, 12, 13, 14, 15 was 19.47 %, 24.22 %, 46.82 %, 81.27 %, 80.91 %, 45.67 %, 23.29 %, 18.12 % respectively. The percentage of class II for teeth 2, 3, 4, 5 12, 13, 14, 15 was 80.53 %, 75.78 %, 53.18 %, 18.73 %, 19.09 %, 54.33 %, 76.71 %, 81.88 % respectively.

7. Diagnostic performance analysis

7.1. The MSF-MPTnet model was reliable

After training, validating, and testing on 1035 PRs, the sensitivity, specificity, accuracy of the MSF-MPTnet deep learning network DenseNet were evaluated using matrix confusion (Table 2). The sensitivity was 0.611–0.988, and the accuracy was 0.890–0.961. The receiver operating characteristic curves (ROC) of Model I and Model II were shown in Fig. 2C, and the AUC value was 0.63–0.72. Therefore, the output performance of MSF-MPTnet model was reliable. The specificity of maxillary molars and second premolars was 0.855–0.987. The specificity of maxillary first premolars was 0.611–0.684.

The intraclass correlation coefficient (ICC) of all the maxillary posterior teeth was shown in Table 1. The ICC of dentists was 0.460–0.690, and it was 0.453–0.664 for radiologists, indicating that the judgments of dentists and radiologists were in low to moderate consistency.

7.2. The accuracy of the MSF-MPTnet model was higher than dentists and radiologists

350 PRs were randomly selected as test dataset and the accuracy of 5 dentists, 5 radiologists and MSF-MPTnet model was compared. The detailed accuracy of the MSF-MPTnet model, dentists and radiologists based on PRs to detect the true contact relationship between MSF and MPT were shown in Fig. 3A. The accuracy of the MSF-MPTnet model was higher than that of dentists and radiologists in maxillary first premolars ($p < 0.05$). The accuracy was 83.4%–87.0 %, 76.2%–76.9 % and 72.9%–73.8 % in MSF-MPTnet model, dentists and radiologists for teeth 2, 3, 4, 5 12, 13, 14, 15 respectively.

The accuracy of class I relationship in MSF-MPTnet model, dentists and radiologists were shown in Fig. 3B. The accuracy of class I relationship was 70.8%–94.6 %, 56.5%–83.1 % and 35.7%–78.1 % in MSF-MPTnet model, dentists and radiologists for teeth 2, 3, 4, 5 12, 13, 14, 15 respectively. The accuracy of class I relationship in MSF-MPTnet model was higher than that of the dentist on the maxillary first premolars and the maxillary left first molar, and higher than radiologists in all the teeth position ($p < 0.05$). The accuracy of class II relationship in MSF-MPTnet model, dentists and radiologists were shown in Fig. 3C. The accuracy of class II relationship was 38.8%–95.1 %, 62.1%–96.9 % and 72.4%–98.8 % in MSF-MPTnet model, dentists and radiologists for teeth 2, 3, 4, 5 12,

Table 2
The Diagnostic Performance Analysis of MSF-MPTnet model in different teeth position.

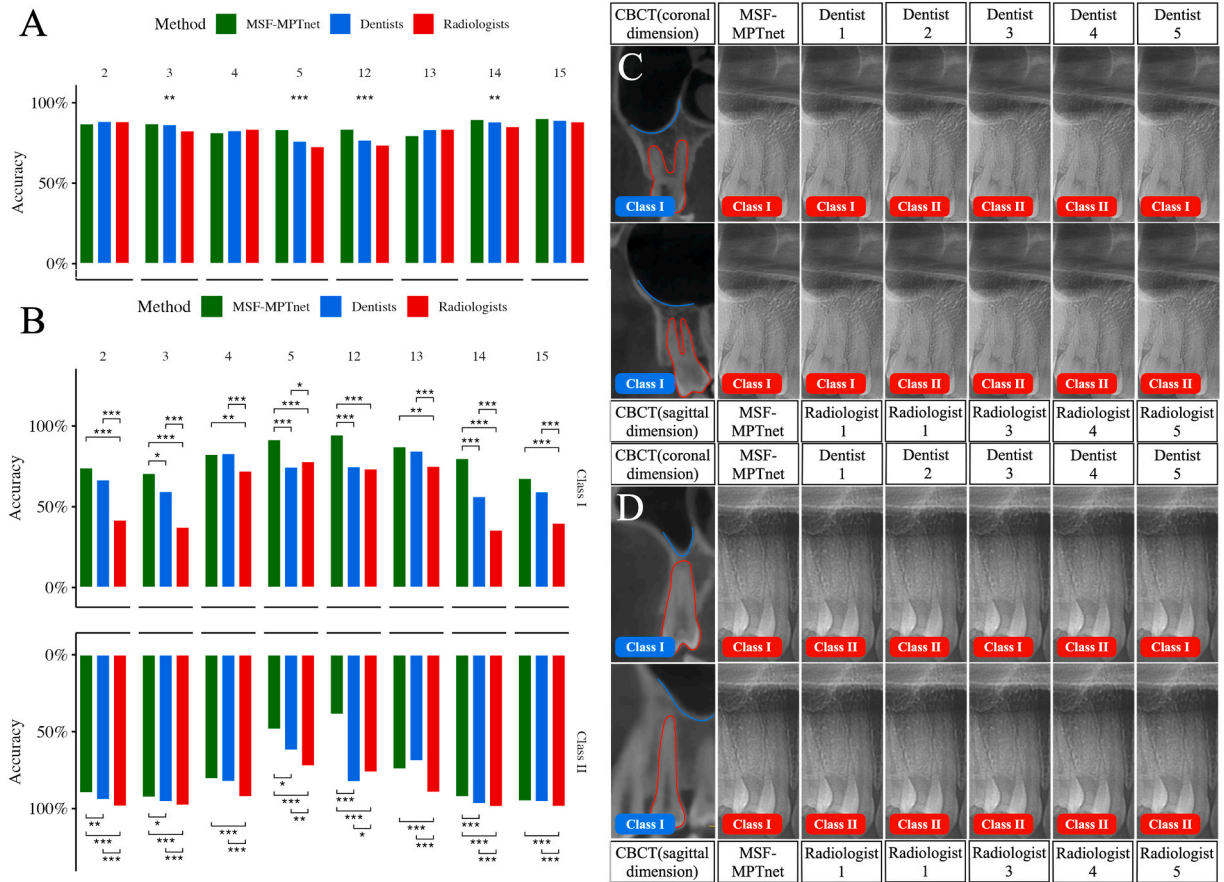| Parameters/Teeth position	Sensitivity	Specificity	Accuracy
2	0.742	0.613	0.870
3	0.708	0.768	0.871
4	0.826	0.763	0.815
5	0.917	0.882	0.834
12	0.945	0.865	0.837
13	0.873	0.701	0.797
14	0.800	0.741	0.897
15	0.677	0.750	0.903

Fig. 3. The accuracy of MSF-MPTnet model was higher than dentists and radiologists. A.Among 3 groups, the accuracy of the MSF-MPTnet model was higher than dentists and radiologists in maxillary first premolars and first molars ($p < 0.05$) B.The accuracy of class I relationship in MSF-MPTnet model was higher than dentists in maxillary first premolars and higher than radiologists in all the teeth position except maxillary right second premolar ($p < 0.05$). No significant difference of the accuracy of class II relationship was found between MSF-MPTnet model and dentists. No significant difference of the accuracy of class II relationship was found between MSF-MPTnet model and radiologists except maxillary left first molar. ($p>0.05$) C.Pseudo class II relationship of dentists and radiologists in assessing maxillary first molars D.Pseudo class II relationship of dentists and radiologists in assessing maxillary first premolars.

13, 14, 15 respectively. A significant difference in the accuracy of class II relationship was found between MSF-MPTnet model and dentists in maxillary right first premolars and the maxillary left first molar ($p < 0.05$). A significant difference in the accuracy of class II relationship was found between MSF-MPTnet model and radiologists.

8. Discussion

Deep learning plays an important role in dentistry for detection of oral cancer, maxillofacial fracture, dental caries and so on. In the present study, it was demonstrated that AI algorithms are capable to detect the relationship between the maxillary sinus floor and maxillary posterior teeth on PRs with an accuracy of at least 89 %. A novel DenseNet-based detection model and deep learning networks based on PRs, named MSF-MPTnet, were successfully established for the first time, and the performance among MSF-MPTnet model, dentists and radiologists was evaluated in detecting the true contact relationship between MSF and MPT. The diagnostic performance analysis showed that the sensitivity, specificity and accuracy of the MSF-MPTnet model were high, indicating that the output performance of the model was reliable. The intraclass correlation coefficient of dentists and radiologists was 0.460–0.690 and 0.453–0.664 respectively, indicating that the judgments of dentists and radiologists regarding the true contact relationship between MSF and MPT based on the same PRs were in low to moderate consistency. Therefore, the MSF-MPTnet model was more stable than dentists and radiologists.

The outline of the maxillary sinus is often difficult to find, even for an experienced dentist. In order to increase the accuracy of dentists and radiologists in this study, they were trained to recognize the anatomy and the outline of maxillary sinus in PRs as stated in the oral radiology book [19]. The tooth segmentation model in PRs was already established in our previous study [20], and the floor of maxillary sinus needs to labeled in this study. Therefore, unlike many previous studies that mainly focused on teeth or maxillary sinus

segmentation [14,21], the present study examined the relationship between MSF and MPT in PRs using a DenseNet-based detection model. DenseNet, a convolutional neural network with dense connectivity structure, is able to learn deeper and more discriminative features from images and has been applied to medical image analysis and has achieved breakthroughs [22]. DenseNet has been effectively validated in publicly available and relevant medical image databases [23]. Therefore, the MSF-MPTnet model can help dentists to evaluate the true contact relationship between MSF and MPT, and has good potential for application in dental practice [24, 25].

Generally, the detecting accuracy of MSF-MPTnet was higher than that of dentists and radiologists, and radiologists had the lowest detection accuracy. This indicated that the output performance of the model was better than dentists and radiologists. Significant difference of accuracy (including class I and class II) was found between MSF-MPTnet, dentists and radiologists in maxillary first premolars and first molars. It was previously reported that the accuracy of class I relationship of MSF and MPT on PRs was 56.1%–85.0 % [26–28]. In this study, the accuracy of class I relationship in radiologists was 35.7%–78.1 %, in dentists the accuracy was 56.5%–84.6 %, and in MSF-MPTnet model the accuracy was 67.7%–94.6 %. Therefore, MSF-MPTnet model increased the accuracy in assessing class I relationship of MSF and MPT on PRs.

It was found in this study on CBCT that class II relationship was the most common in maxillary molars, and class I relationship was the most common in maxillary first premolars. The percentage of class I and II relationship was nearly half to half in maxillary second premolars. This indicated that the roots of maxillary first premolars have little relationship with the MSF, and molars showed greater proximity to MSF than premolars, which was coincident with previous studies [29,30]. Therefore, special consideration should be given to maxillary molars when accepting dental therapy. In addition, no significant differences was found between the left and right MPTs, which was also in agreement with previous studies.

The accuracy of class I relationship of radiologists was relatively low compared to dentists and the MSF-MPTnet model, especially in the maxillary molars. Furthermore, it was found that there were pseudo class II relationship of dentists and radiologists in assessing maxillary first premolars and molars in PRs, while the model acquired the correct class I relationship affirmed by the CBCT (Fig. 3C and D). Therefore, PRs were shown to overestimate the position of MPT by dentists and radiologists who suggested it was in the sinus when it was not. Previous results showed a high level of disagreement between CBCT and PRs when the root is laterally projecting over the sinus [27,31]. The superimposition of anatomic structures, distortion, and the absence of cross-sectional information will cause the pseudo-contact relationship between MSF and MPT on PRs. Therefore, the model for detecting the true contact relationship between MSF and MPT based on PRs was generally successful. The model could serve as assistant of dentists and radiologists and improve the detecting accuracy. Evidently, when PRs shows a distinct distance between MSF and MPT by the MSF-MPTnet model, it is unnecessary to order a CBCT. In this situation, the frequency of CBCT use was reduced.

There were no significant difference of accuracy between MSF-MPTnet and dentists in assessing class II relationship with a relatively high accuracy, and relatively low accuracy was found in maxillary first premolars. The accuracy of class II relationship of MSF-MPTnet model in maxillary first premolars was 38.8%–48.5 %, which might be related to the relatively low percentage of class II relationship in maxillary first premolars (18.73%–19.09 %) limited the effectiveness of model training. If the root tip is in close contact with MSF, there is a high risk of sinus perforation during extractions or endodontic surgery. Dental diseases including periapical or periodontal infections of MPT, can spread to the MS and lead to odontogenic sinusitis, it was found that over 50 % of maxillary sinusitis were of dental etiology [3,32]. Root protrusion into MS may induce root resorption or tipping during orthodontic treatment [4]. Therefore, CBCT should be ordered for clarification when a class II relationship between MSF and MPT is found.

Some limitations should be mentioned in the present study. The relatively small training dataset might lead to deviations in the conclusions drawn, and the training dataset needs to be enlarged to increase the accuracy of the MSF-MPTnet model. In the future, we need to expand the dataset to enhance the accurary of the MSF-MPTnet in predicting Class II relationships. By considering the proportional length of tooth roots in panoramic and CBCT images, we can train the model to predict the contact relationship between MPT and MSF. Additionally, we can quantify the length of tooth roots specifically in panoramic images, enabling the sub-model to better serve clinical purposes. This will aid the model in more accurately understanding the position and relationships of tooth roots in different images, providing more precise information for clinical decision-making.

9. Conclusions

This study established a new reliable DenseNet-based artificial intelligence detection model named MSF-MPTnet, which can assist dentists and radiologists in assessing the true contact relationship between MSF and MPT based on PRs. MSF-MPTnet model could increase detecting accuracy of the relationship between MSF and MPT, minimize pseudo contact relationship and reduce frequency of CBCT use.

Ethics approval number

Ethic committee of Stomatology Hospital, Zhejiang University School of Medicine.

Funding

Zhejiang Provincial Public Welfare Research Program, China (Grant Number LTGY23H140007); Clinical research project of Chinese Orthodontic Society, China (Grant Number COS–C2021-09); The Research and Development Project of Stomatology Hospital Zhejiang University School of Medicine, China (Grant Number RD2022YFZD01)

Statement of clinical relevance

The close relationship of the maxillary posterior teeth and maxillary sinus floor may result in various complications such as odontogenic sinusitis, perforation, formation of oroantral fistula, or root displacement into the MS.

CRediT authorship contribution statement

Wanghui Ding: Writing – review & editing, Methodology, Funding acquisition, Conceptualization. **Yindi Jiang:** Project administration, Investigation, Formal analysis, Data curation. **Gaozhi Pang:** Project administration, Methodology, Formal analysis, Data curation. **Ziang Liu:** Writing – review & editing, Conceptualization. **Yuefan Wu:** Investigation, Formal analysis. **Jianhua Li:** Writing – review & editing, Conceptualization. **Fuli Wu:** Writing – review & editing, Conceptualization.

Declaration of competing interest

The authors declare that they have no known competing financial interests or personal relationships that could have appeared to influence the work reported in this paper.

References

[1] B. Shrestha, R. Shrestha, H. Lu, Z. Mai, L. Chen, Z. Chen, et al., Relationship of the maxillary posterior teeth and maxillary sinus floor in different skeletal growth patterns: a cone-beam computed tomographic study of 1600 roots, Imaging Sci Dent 52 (2022) 19–25.

[2] S.M. Kim, Definition and management of odontogenic maxillary sinusitis, Maxillofac Plast Reconstr Surg 41 (2019) 13.

[3] M. Maillet, W.R. Bowles, S.L. McClanahan, M.T. John, M. Ahmad, Cone-beam computed tomography evaluation of maxillary sinusitis, J. Endod. 37 (2011) 753–757.

[4] A. Shokri, S. Lari, F. Yousef, L. Hashemi, Assessment of the relationship between the maxillary sinus floor and maxillary posterior teeth roots using cone beam computed tomography, J. Contemp. Dent. Pract. 15 (2014) 618–622.

[5] W. Sun, K. Xia, X. Huang, X. Cen, Q. Liu, J. Liu, Knowledge of orthodontic tooth movement through the maxillary sinus: a systematic review, BMC Oral Health 18 (2018) 91.

[6] H. Lee, A. Badal, A review of doses for dental imaging in 2010-2020 and development of a web dose calculator, Radiol Res Pract 2021 (2021) 6924314.

[7] M. Marcu, M. Hedesiu, B. Salmon, R. Pauwels, A. Stratis, A.C.C. Oenning, et al., Estimation of the radiation dose for pediatric CBCT indications: a prospective study on ProMax3D, Int. J. Paediatr. Dent. 28 (2018) 300–309.

[8] Y.H. Jung, B.H. Cho, J.J. Hwang, Comparison of panoramic radiography and cone-beam computed tomography for assessing radiographic signs indicating root protrusion into the maxillary sinus, Imaging Sci Dent. 50 (2020) 309–318.

[9] N. Ahmed, M.S. Abbasi, F. Zuberi, W. Qamar, M.S.B. Halim, A. Maqsood, et al., Artificial intelligence techniques: analysis, application, and outcome in dentistry-A systematic review, BioMed Res. Int. 2021 (2021) 9751564.

[10] N. Banar, J. Bertels, F. Laurent, R.M. Boedi, J. De Tobel, P. Thevissen, et al., Towards fully automated third molar development staging in panoramic radiographs, Int J Legal Med 134 (2020) 1831–1841.

[11] J. Krois, T. Ekert, L. Meinhold, T. Golla, B. Kharbot, A. Wittemeier, et al., Deep learning for the radiographic detection of periodontal bone loss, Sci. Rep. 9 (2019) 8495.

[12] J.H. Lee, D.H. Kim, S.N. Jeong, S.H. Choi, Detection and diagnosis of dental caries using a deep learning-based convolutional neural network algorithm, J. Dent. 77 (2018) 106–111.

[13] D.V. Tuzoff, L.N. Tuzova, M.M. Bornstein, A.S. Krasnov, M.A. Kharchenko, S.I. Nikolenko, et al., Tooth detection and numbering in panoramic radiographs using convolutional neural networks, Dentomaxillofacial Radiol. 48 (2019) 20180051.

[14] J.Y. Cha, H.I. Yoon, I.S. Yeo, K.H. Huh, J.S. Han, Panoptic segmentation on panoramic radiographs: deep learning-based segmentation of various structures including maxillary sinus and mandibular canal, J. Clin. Med. 10 (2021).

[15] R. Kuwana, Y. Ariji, M. Fukuda, Y. Kise, M. Nozawa, C. Kuwada, et al., Performance of deep learning object detection technology in the detection and diagnosis of maxillary sinus lesions on panoramic radiographs, Dentomaxillofac Radiol 50 (2021) 20200171.

[16] J. Xu, S. Wang, Z. Zhou, J. Liu, X. Jiang, X. Chen, Automatic CT image segmentation of maxillary sinus based on VGG network and improved V-Net, Int. J. Comput. Assist. Radiol. Surg. 15 (2020) 1457–1465.

[17] K.F. Hung, Q.Y.H. Ai, A.D. King, M.M. Bornstein, L.M. Wong, Y.Y. Leung, Automatic detection and segmentation of morphological changes of the maxillary sinus mucosa on cone-beam computed tomography images using a three-dimensional convolutional neural network, Clin Oral Investig 26 (2022) 3987–3998.

[18] P. Zeng, R. Song, Y. Lin, H. Li, S. Chen, M. Shi, et al., Abnormal maxillary sinus diagnosing on CBCT images via object detection and 'straight-forward' classification deep learning strategy, J. Oral Rehabil. 50 (2023) 1465–1480.

[19] S.C. White, M.J. Pharoah, Oral Radiology-E-Book: Principles and Interpretation, Elsevier Health Sciences, 2014.

[20] F. Zhang, J. Zhu, P. Hao, F. Wu, Y. Zheng, BDU-net: toward accurate segmentation of dental image using border guidance and feature map distortion, Int. J. Imag. Syst. Technol. 32 (2022) 1221–1230.

[21] C. Sheng, L. Wang, Z. Huang, T. Wang, Y. Guo, W. Hou, et al., Transformer-based deep learning network for tooth segmentation on panoramic radiographs, J. Syst. Sci. Complex. (2022) 1–16.

[22] Z. Zhou, J. Shin, L. Zhang, S. Gurudu, M. Gotway, J. Liang, Fine-tuning convolutional neural networks for biomedical image analysis: actively and incrementally, Proc IEEE Comput Soc Conf Comput Vis Pattern Recognit. 2017 (2017) 4761–4772.

[23] T. Zhou, X. Ye, H. Lu, X. Zheng, S. Qiu, Y. Liu, Dense convolutional network and its application in medical image analysis, BioMed Res. Int. 2022 (2022) 2384830.

[24] J.R. Gardner, P. Upchurch, M.J. Kusner, Y. Li, K.Q. Weinberger, K. Bala, et al., Deep Manifold Traversal: Changing Labels with Convolutional Features, 2015 arXiv preprint arXiv:151106421.

[25] L.A. Gatys, A.S. Ecker, M. Bethge, A Neural Algorithm of Artistic Style, arXiv Preprint arXiv:150806576, 2015.

[26] B.A. Hassan, Reliability of periapical radiographs and orthopantomograms in detection of tooth root protrusion in the maxillary sinus: correlation results with cone beam computed tomography, J. Oral Maxillofac. Res. 1 (2010) e6.

[27] C. Kalkur, A.P. Sattur, K.S. Guttal, V.G. Naikmasur, K. Burde, Correlation between maxillary sinus floor topography and relative root position of posterior teeth using Orthopantomograph and Digital Volumetric Tomography, Asian J. Med. Sci. 8 (2017) 26–31.

[28] L.J. Lopes, T.O. Gamba, J.V. Bertinato, D.Q. Freitas, Comparison of panoramic radiography and CBCT to identify maxillary posterior roots invading the maxillary sinus, Dentomaxillofacial Radiol. 45 (2016) 20160043.

[29] Y. Gu, C. Sun, D. Wu, Q. Zhu, D. Leng, Y. Zhou, Evaluation of the relationship between maxillary posterior teeth and the maxillary sinus floor using cone-beam computed tomography, BMC Oral Health 18 (2018) 164.

[30] S. Razumova, A. Brago, A. Howijieh, A. Manvelyan, H. Barakat, M. Baykulova, Evaluation of the relationship between the maxillary sinus floor and the root apices of the maxillary posterior teeth using cone-beam computed tomographic scanning, J. Conserv. Dent. 22 (2019) 139–143.

[31] M. Shahbazian, C. Vandewoude, J. Wyatt, R. Jacobs, Comparative assessment of panoramic radiography and CBCT imaging for radiodiagnostics in the posterior maxilla, Clin Oral Investig 18 (2014) 293–300.

[32] X. Zhang, Y. Li, Y. Zhang, F. Hu, B. Xu, X. Shi, et al., Investigating the anatomical relationship between the maxillary molars and the sinus floor in a Chinese population using cone-beam computed tomography, BMC Oral Health 19 (2019) 282.